

KINETICS OF POTASSIUM CATALYZED GASIFICATION

P. Knoer and H. W. Wong. Exxon Research and Engineering Co., Baytown Research and Development Division, P. O. Box 4255, Baytown, Texas 77520.

Commercial applications of the potassium catalyzed coal gasification reaction (CCG) are envisioned to include high pressure (2000 to 4000 kPa) and high concentrations of hydrogen in the gasification reactor (1, 2, 3). Published literature regarding CCG, however, report studies conducted at low pressure or with low concentrations of hydrogen or both (4, 5, 6). The present study was conducted to investigate the gasification reaction under commercially representative conditions. Thus, pressure was varied from 100 to 3500 kPa and hydrogen concentration was varied from 0 to 60%. Other reaction conditions, such as temperature and catalyst loading, were also varied in this study to check published results at these more representative conditions. The data from this study were combined with mechanistic information from the literature (6). Only one kinetic model was found which fit both the data and the literature mechanism. The two adjustable constants for this model were regressed using over 1200 pieces of data. The overall fit between the model and the data is very good.

Experimental Apparatus

This experimental program was carried out using a one atmosphere mini-fluid bed reactor and a fixed bed reactor capable of operating at high pressure. The atmospheric pressure unit was used to study variations in catalyst loading and temperature. These studies were conducted using both H₂O only and H₂O/H₂ mixtures, using chars from steady state pilot plant operations and chars prepared by devolatilization in the laboratory.

A schematic diagram of the mini-fluid bed reactor unit is shown in Figure 1. The reactor portion of the unit consists of a 0.6 cm I.D. quartz U-tube inside a hot steel block. Water is fed to the U-tube using a small syringe pump and is vaporized in the reactor. Argon or hydrogen gas is also fed to the unit. Ceramic beads are placed in the inlet leg of the U-tube to enhance the vaporization of water and to help disperse the gas flow. The exit gases from the reactor flow into an oxidizer where all carbon species are converted to carbon dioxide. After condensing any unreacted steam, the gas stream is bubbled through a sodium hydroxide solution where the amount of total carbon converted is automatically monitored by measuring the conductivity of the solution.

The argon or hydrogen gas fed to the mini-fluid bed serves to fluidize the char particles. The gas rate is typically about 40 cc/min STP which is equivalent to about 7 cm/sec linear superficial velocity in the reactor at 700°C. The minimum fluidizing velocity of the char particles is 3-4 cm/sec. Char sample sizes varied from 0.25 grams to 1.00 gram in the minifluid bed. The water feed rate ranged from 0.2 to 2.5 ml/hour.

The fixed bed reactor was used primarily to study pressure effects. All runs in the fixed bed were made at 700°C using laboratory prepared char. Variations were made in feed gas composition and flow rate. A simplified flow diagram of the fixed bed unit is shown in Figure 2. The unit consists of a high pressure water pump, steam generator, fixed bed reactor, condenser for unreacted steam, gas chromatographs, and dry gas flow measurement system.

The reactor itself is a one-inch Schedule 80 type 316 stainless steel pipe. The pipe holds a char sample inside a split tube furnace.

Effect of Varying Potassium-to-Carbon Ratio

If the overall carbon conversion is altered in the CCG reactor, the ratio of potassium-to-carbon (K/C) in the reactor will change as well. Therefore, the effect of catalyst loading on kinetics must be known in order to be able to optimize initial catalyst loading as well as overall carbon conversion for the CCG process. Experiments were conducted in the atmospheric mini-fluid bed reactor to determine the effect of carbon conversion and catalyst loading on the gasification rate.

Plotting the initial gasification rates against the water soluble K/C ratio reveals an approximately linear relationship between the two as shown in Figures 3 and 4. This is consistent with the earlier findings by others (6).

This suggests that the rate of gasification is proportional to the concentration of a (C-K) species rather than carbon or potassium concentrations per se. At high carbon concentrations and low K/C ratios, the concentration of the (C-K) species is proportional to the concentration of (K) since there is an overabundance of (C). The gasification rate thus appears to be independent of carbon concentration (i.e., zero order kinetics). At low carbon concentrations and high K/C ratios, there is an overabundance of (K). The gasification rate will then appear to be first order with respect to carbon. From studies of pilot plant chars, the demarcation between high and low K/C ratios appears to be about 0.2 mole C/mole water soluble potassium.

Variation of Reaction Temperature

The dependence of gasification rate on temperature was studied in the mini-gasifier, both with and without H₂ in the feed gas.

Figure 5 shows the measured reaction rates as a function of temperature for experiments both with and without H₂ in the reactor. The apparent temperature dependence changes as the composition of the gas fed to the reactor changes. From Figure 4 it is seen that for H₂O + H₂ in the feed gas, gasification rate is very sensitive to temperature changes. Gasification rate approximately halves for each 25°C drop in reactor temperature below 700°C.

There is an interaction between feed gas composition and apparent temperature dependence because the mini-reactor is an integral reactor. For example, when pure steam is introduced at the bottom of the bed of char, a mixture of $H_2O + H_2$ issues from the top of the bed. As the rate of reaction changes, the gas composition at various locations in the reactor changes even though the feed gas remains the same. Therefore, as temperature changes, some of the change in rate is due to activation energy, but some of the change is due to gas composition. A reactor model which performs an integration over the bed is required to account for both effects. Our modeling work discussed in the next section of this report has identified the true activation energy as about 50 kcal/g mole.

Gasification Rate Expression

During an earlier phase of research on the CCG process, a screening of gasification reaction rate models was reported by Vadovic and Eakman (5). In this screening, all combinations of from one to four inhibition terms involving the partial pressures of H_2 , CO , H_2O , and the cross products of the partial pressures of H_2 and CO , and H_2 and H_2O were tested in the denominator of the gasification rate expression. In all, they tested thirty models. Those models which gave negative coefficients on regression were discarded as being physically unreal. Four additional models were discarded because they gave an infinite rate for a pure steam environment. Of the thirty models tested, three models remained which gave good fit to their data. These three are listed below.

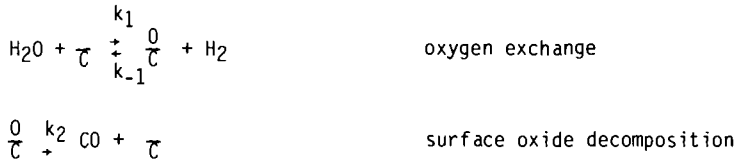
$$(A) \quad r_G = \frac{k(P_{H_2O} - P_{CO}P_{H_2}/2KG)}{P_{H_2} + 0.1775 P_{H_2O}}$$

$$(B) \quad r_G = \frac{k(P_{H_2O} - P_{CO}P_{H_2}/2KG)}{P_{H_2} + 0.210 P_{H_2}P_{CO} + 0.0595 P_{H_2O}}$$

$$(C) \quad r_G = \frac{k(P_{H_2O} - P_{CO}P_{H_2}/2KG)}{P_{H_2} + 1.26 P_{CO} + 0.349 P_{H_2O}}$$

For their screening of gasification rate models, Vadovic and Eakman used data from runs in which only pure steam was fed to the bed of coal char. Mixtures of H_2O and H_2 or H_2O , H_2 , and CO were introduced and studied in the present program.

In addition to the empirical data, mechanistic considerations were used to discriminate among the three models for catalytic gasification kinetics. Several mechanisms have been proposed for the steam-carbon reaction in the past (7). Recent work by Mims and Pabst (6) indicated that the overall gasification kinetics are consistent with a simple surface oxide mechanism:



With the larger data base and the proposed mechanism, it was possible to better distinguish among the three rate models identified earlier. Only Model A was found to be consistent with both the mechanism studies and the new data. This model is shown in general form below:

$$r_G = \frac{k(P_{\text{H}_2\text{O}} - P_{\text{H}_2}P_{\text{CO}}/2K_G)}{P_{\text{H}_2} + b P_{\text{H}_2\text{O}}} \quad (1)$$

r_G = the rate of gasification in moles per hour per ft³ of reactor

K_G = the equilibrium constant for steam and β -graphite

P_i = the partial pressure of component i in the reactor

k = the rate constant; it contains the catalyst loading and temperature dependence.

Parameter Estimation for the Gasification Reaction

A total of 28 successful fixed bed runs were made at pressures ranging from 100 to 3500 kPa, H₂ flows ranging from 0 to 1.0 moles per hour, CO flows ranging from 0 to 0.17 moles per hour and steam flows ranging from 0.3 to 1.3 moles per hour. It was observed that the total gas make and gas composition changed during the runs as carbon was depleted from the bed. It was also observed that the methane and carbon dioxide were nearly in chemical equilibrium with the other gas phase components for the conditions studied.

A combination of kinetic constants k and b in Equation 1 were sought which would make the predictions of the fixed bed model best fit the fixed

bed data. Best fit is defined by a small deviation between predicted and observed molar flow rates. Thus, one expression of the objective function would be as follows:

$$\text{minimize } s^2 = \sum_k \sum_j \sum_i (\tilde{N}_{ijk} - N_{ijk})^2 \quad (2)$$

where,

S = the sum of the squares of the deviations

\tilde{N}_{ijk} = a predicted molar flow rate

N_{ijk} = an observed molar flow rate

i = a particular gas component (H_2 , CO , CO_2 , CH_4 , or H_2O)

j = a particular level of carbon in the fixed bed reactor

k = a particular fixed bed reactor run

Hunter (8) has shown that use of this objective function will yield the maximum likelihood estimates for k and b only if the following three criteria are met:

- (1) The measurement errors on each of the five gas species are normally distributed and these errors are independent.
- (2) The variances on the measurement errors of all of the five gas species are identical.
- (3) There is no correlation between the measurement errors for any two gas species.

From the design of the experiment we know that the measurements on the four fixed gases were related in that they were all sampled simultaneously by the gas chromatograph and the composition was normalized. Therefore, an error in the measurement of any one of the four fixed gases would be distributed among the other three fixed gases as well. Furthermore, any error in the measurement of CO or CO_2 would result in an error in the measurement of H_2O as well since H_2O yield was calculated by oxygen balance. As a result of these considerations, equation 2 was not used as the objective function for this study.

Box and Draper (9) have derived the following objective function for use in cases where unquantified covariance exists in the experimental measurements:

$$\text{minimize } \Delta = \det | S_{nm} |$$

where,

Δ = the determinant of the 5×5 matrix composed of elements S_{nm}

and,

$$S_{nm} = \sum_k \sum_j (\tilde{N}_{njk} - N_{njk})(\tilde{N}_{mjk} - N_{mjk})$$

where,

n,m = particular gas components
j,k = as above.

Hunter (8) recommends the use of this objective function when covariance might exist in the experimental measurements.

Rosenbrock's hill climbing method (10) was used to search for the optimum values of k and b in equation 1. For each set of k and b, the fixed bed reactor model equations were numerically integrated 28 times; i.e., once for each fixed bed reactor run being estimated. For each of the 28 fixed bed reactor runs, comparisons between calculated and observed molar flow rates were made for 8 to 10 different levels of carbon in bed. With five different gas species being estimated, there were over 1200 comparisons made for each guess of a k,b pair. For each guess, the appropriate cross products of deviations were calculated and accumulated to form the 5 X 5 matrix of elements S_{nm} . The determinant of this matrix was calculated and used by the Rosenbrock routine to make a new guess at k and b.

Results of the Regression

The initial guesses for k and b were taken from the results of Vadovic and Eakman (5). For 700°C and the K/C ratio used these were as follows:

$$k = 0.0204$$

$$b = 0.1775$$

The routine returned the following values:

$$k = 0.0173$$

$$b = 0.2080$$

Figures 6 through 10 are parity plots of the predicted and observed values of the molar flow rates of H₂, CO, CO₂, CH₄, and H₂O. The parity plots show that the fixed bed reactor model does a good job of predicting all of the gas species from the fixed bed reactor runs over a wide variety of conditions with the exception of CH₄. A slight overprediction of CH₄ yield is observed.

Conclusions

The potassium catalyzed gasification of Illinois No. 6 bituminous coal was found to fit a Langmuir-Hinshelwood type kinetic model. This model provides a good fit to fixed bed and miniature fluid bed data over pressures

ranging from atmospheric to 3500 kPa and over broad ranges of gas composition. The model closely predicted the observed flow rates of each specie in the product gas over a range of an order of magnitude or more. This model is consistent with the surface oxide mechanism for the steam-carbon reaction which was proposed in earlier literature. A sophisticated statistical regression technique was used to choose the two adjustable constants for this model by comparison with over 1200 pieces of data.

The kinetic constants were regressed from data taken over the range of practical commercial interest. This kinetic model may be combined with independently verified correlations for bubble growth and mass transfer in a fluidized bed and used directly to study larger pilot plant data or scale-up issues.

ACKNOWLEDGEMENT

This work was supported by the United States Department of Energy under Contract No. ET-78-C-01-2777 and by the Gas Research Institute.

REFERENCES

1. N. C. Nahas and J. E. Gallagher, Jr., "Catalytic Gasification Predevelopment Research," Proceedings of the Thirteenth Intersociety Energy Conversion Engineering Conference, (August 1978).
2. B. T. Fant and C. A. Euker, Jr., "Exxon's Catalytic Coal Gasification Process," Presented to The First International Research Conference, (June 9-12, 1980).
3. D. Hebden and H. J. F. Stroud, "Coal Gasification Processes," in Chemistry of Coal Utilization Second Supplementary Volume, M. A. Elliot ed., (1981), pp. 1649-1650.
4. H. G. Hipkin, Carbon-Steam System at Low Temperatures and Under Pressure, PhD Thesis, M.I.T. (1951).
5. C. J. Vadovic and J. M. Eakman, "Kinetics of Potassium Catalyzed Gasification," presented at the meeting of the American Chemical Society (September, 1978).
6. C. A. Mims and J. K. Pabst, "Alkali Catalyzed Carbon Gasification II. Kinetics and Mechanism," presented at the meeting of the American Chemical Society (August, 1980).
7. P. L. Walker, Jr., F. Rusinko, Jr., and L. G. Austin, Advances in Catalysis XI, (1959).
8. W. G. Hunter, "Estimation of Unknown Constants From Multi-response Data," I & E C Fundamentals, Vol. 6, (1967), pp. 461-463.
9. G.E.P. Box and N. R. Draper, Biometrika, V52, (1965), p. 355.
10. H. H. Rosenbrock, "An Automatic Method for Finding the Greatest or Least Value of a Function," Computer J., 3 (1960).

FIGURE 1
SCHEMATIC OF MINI-FLUID BED REACTOR UNIT

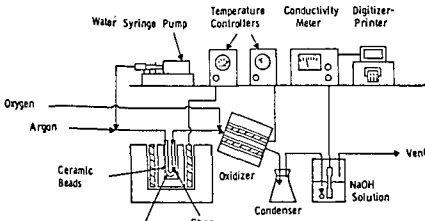


FIGURE 2
SIMPLIFIED FLOW DIAGRAM OF BENCH SCALE GASIFICATION UNIT

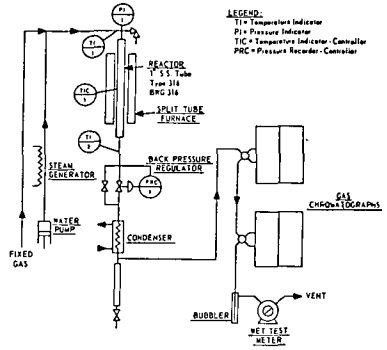


FIGURE 3
GASIFICATION RATE INCREASES LINEARLY WITH (K/C) RATIO

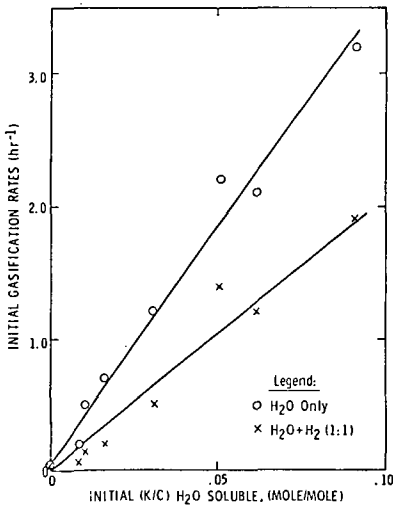


FIGURE 4
EFFECT OF CATALYST LOADING ON GASIFICATION

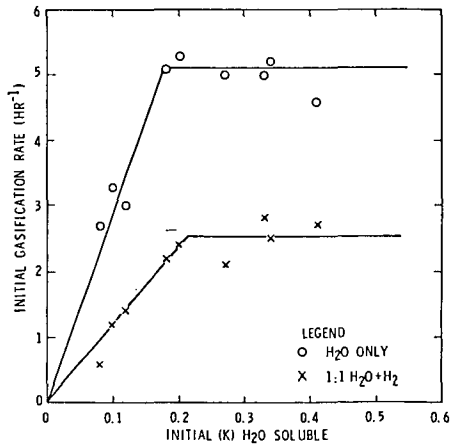
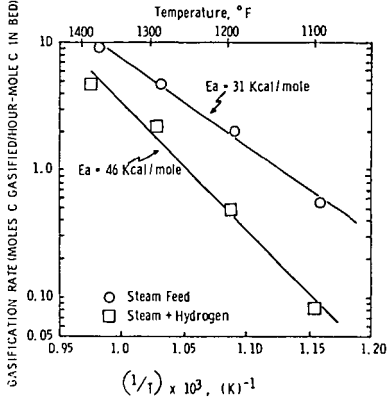


FIGURE 5

APPARENT ACTIVATION ENERGY DEPENDS ON
FEED GAS COMPOSITION



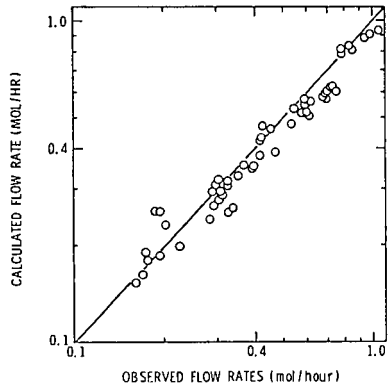
808-4-5-22

808-12-1131

808-12-1130

FIGURE 6

CALCULATED AND OBSERVED FLOW RATES OF HYDROGEN



808-12-1132

FIGURE 7

CALCULATED AND OBSERVED FLOW RATES OF CARBON MONOXIDE

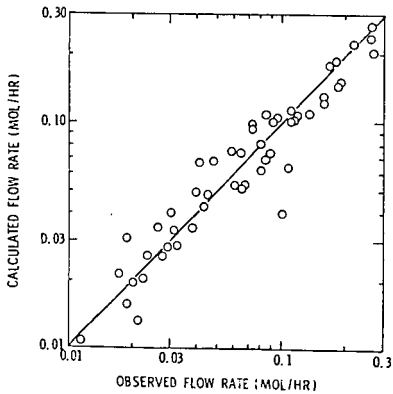


FIGURE 8

CALCULATED AND OBSERVED FLOW RATES OF CARBON DIOXIDE

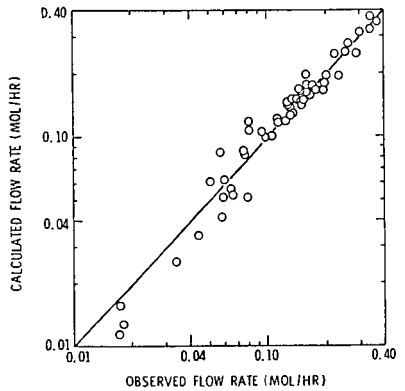


FIGURE 9
CALCULATED AND OBSERVED FLOW RATES FOR METHANE

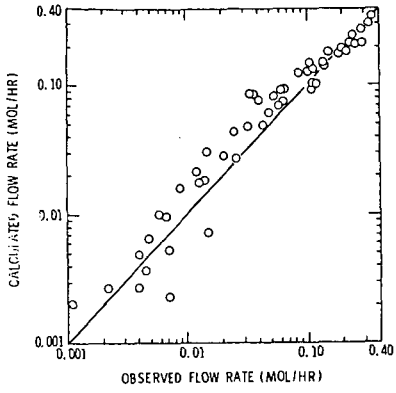


FIGURE 10
CALCULATED AND OBSERVED FLOW RATES FOR STEAM

